

DISTANCES FROM SURFACE BRIGHTNESS FLUCTUATIONS

JOHN P. BLAKESLEE

*California Institute of Technology, M.S. 105-24,
Pasadena, CA 91125; jpb@astro.caltech.edu*

EDWARD A. AJHAR

*National Optical Astronomy Observatories, P.O. Box 26732,
Tucson, AZ 85726; ajhar@noao.edu*

AND

JOHN L. TONRY

*University of Hawaii, 2680 Woodlawn Drive,
Honolulu, HI 96822; jt@avidya.ifa.hawaii.edu*

1. Introduction

The practice of determining galaxy distances from the amplitude of their spatial fluctuations in surface brightness began with the work of Tonry & Schneider (1988), who developed the method in detail and made its initial application to estimating elliptical galaxy distances. While several articles over the past decade have included some review material (e.g., Jacoby *et al.* 1992; Tonry 1996; Tonry *et al.* 1997, hereafter SBF-I), this is the first intended as a comprehensive review of the surface brightness fluctuation (SBF) method.

The SBF method is conceptually quite simple, the basic idea being that nearby (but unresolved) star clusters and galaxies appear “bumpy,” while more distant ones appear smooth. This is quantified via a measurement of the Poisson fluctuations in the number of unresolved stars (in an image of an elliptical galaxy, for instance) encompassed by a CCD pixel. If N is the mean number of stars per pixel and \bar{f} is the mean flux per star, then the mean pixel intensity is $N\bar{f}$ and the variance is $N\bar{f}^2$. Dividing the observed variance by the observed mean yields \bar{f} , which decreases inversely with the square of the distance (d^{-2}). If the corresponding luminosity \bar{L} happens to be a standard candle, the distance follows directly: $d^2 = \bar{L}/4\pi\bar{f}$.

In practice, the measurement is complicated by the fact that adjacent pixels in real CCD images are correlated through convolution with the point spread function (psf) due to the atmosphere and telescope optics. One must therefore determine the variance from the amplitude of the image power spectrum on the scale of the psf. As only celestial sources suffer psf-blurring, this is a mixed blessing, making it possible to remove all noise which does not favor this scale. Examples include noise due to photon counting statistics and CCD read noise.

A further complication is that \bar{L} is not by itself a standard candle in optical bandpasses. However, both theory and observation indicate that it varies in a simple, predictable manner among old stellar populations. The most widely used version of the SBF method employs a standard candle constructed from a linear combination of \bar{M}_I and broad-band ($V-I$) color (e.g., Tonry 1991; SBF-I; Ajhar *et al.* 1997), where \bar{M}_I is the absolute magnitude of \bar{L} in the Kron-Cousins I -band.

Being the ratio of the second and first moments of the stellar luminosity function, \bar{L} is the luminosity-weighted average stellar luminosity (Tonry & Schneider 1988). It is therefore weighted towards the brightest stars in a population; for evolved populations, these are red giant branch (RGB) stars. Since RGB stars are red, SBF magnitudes are red; $\bar{m}_V - \bar{m}_I \approx 2.4$ is a typical SBF color for an elliptical galaxy (Tonry *et al.* 1990, hereafter TAL90). It was for this reason, as well as its relative insensitivity to stellar population differences, that \bar{m}_I was the magnitude of choice for the ‘‘SBF Survey of Galaxy Distances’’ (SBF-I).

The following section describes the technical details and difficulties involved in the SBF method, primarily as applied in the I -band SBF Survey but including approaches used by other authors. Section 3 then discusses the theoretical calibration of the method and various stellar population effects. Details on the data sample, empirical calibration, and results of the SBF Survey are given in Section 4, including comparisons with other methods and constraints on the Hubble constant. Sections 5–6 describe other optical and near-infrared SBF distances measured from the ground, and Section 7 discusses the recent and exciting results with the *Hubble Space Telescope* (*HST*). Section 8 evaluates the strengths, shortcomings, universality, and applicability of the SBF method, and the final section forecasts what the future may hold for it.

2. Measuring the Surface Brightness Fluctuations

Ajhar *et al.* (1998) give a complete presentation of SBF theory and the analysis techniques used in the ground-based I -band survey. Here, we summarize the method and refer the reader to that work for further details.

The ultimate goal for a galaxy image suitable for SBF measurement is that the pixel-to-pixel fluctuations be dominated by the galaxy’s stellar Poisson statistics rather than by flattening errors, CCD artifacts, photon statistics, *etc.* Consequently, successful SBF observations require extraordinary care and planning. Typically, sufficient CCD calibration requires bias and dark frames, high signal-to-noise (S/N) flat fields, and, for thinned CCDs, high signal-to-noise fringe frames. Even “small” amplitude fringing of $\lesssim 1\%$ must be removed for accurate fluctuation measurements because it can have significant power on the scale of the psf. We have found fringe patterns to be remarkably stable and removable from galaxy images by subtracting the fringe frame, appropriately scaled to the observation.

Under nominal observing conditions, the exposure time on a galaxy is dictated by (a) the SBF amplitude \bar{m} (based on its expected distance) and (b) the sensitivity of the detector. Fundamentally, the exposure time must be long enough so that the photon shot noise per pixel is less than the stellar surface brightness fluctuations. The approximate break-even point occurs when one photon is collected per giant star of brightness \bar{m} . In this way, the exposure time is given by

$$t = \frac{S}{N} 10^{0.4(\bar{m}-m_1)}, \quad (1)$$

where m_1 is the magnitude yielding 1 detected photoelectron per second, and S/N is the desired signal-to-noise ratio. One normally strives to collect $\sim 5\text{--}10 e^-$ per \bar{m} star (or $S/N \sim 5\text{--}10$). The general observation procedure is to take 3–10 exposures of 300–600s each, dithering each exposure by $\sim 5''$ perpendicular to the parallel clock direction of the CCD to improve flattening and the removal of fringe patterns and CCD defects.

Because the I -band SBF calibration is sensitive to the $(V-I)$ color of the galaxy, precise color measurements are required for a reliable distance measurement. As a result, sufficient time must be spent observing standard stars to ensure a precise photometric calibration.

Once the data are collected and the initial CCD calibration is complete (including fringe removal, if necessary), we register and stack the series of I -band galaxy observations and remove cosmic ray events. The final I -band image is used with a V -band image, usually observed at the same time, to determine the $(V-I)$ color of the galaxy. We first mask obvious point sources, background galaxies, and any dusty regions in the galaxy. We estimate the sky levels by fitting the outer regions of the galaxy to an $r^{1/4}$ law profile plus a constant sky offset. Based on these sky estimates, we compute $(V-I)$ colors for the galaxy as a function of radius, corresponding to the \bar{m} measurements to be made.

The next step is to fit and remove the galaxy. First, we mask all the obvious objects and any dust. Next, we fit elliptical isophotes to the sky-

subtracted galaxy image and build a model of the galaxy pixel-by-pixel by interpolating between fitted ellipses. Finally, we subtract the model from the data image. The residual large-scale deviations from a flat background are then fitted and subtracted from the image. We note that this technique does corrupt the lowest wavenumbers of the image power spectrum. In addition, imperfect flattening and fringe removal potentially corrupt the low wavenumbers as low spatial frequency power may be introduced into the data at that stage of the reduction. However, this is irrelevant in the end because we omit low wavenumbers from the determination of \overline{m} .

While some authors (Pahre & Mould 1994) have used a similar method to remove the mean galaxy light, others have employed some kind of adaptive filter. Lorenz *et al.* (1993) used a Laplace filter to subtract galaxy light from the image. Neilsen *et al.* (1997) employed a Butterworth filter in Fourier space to remove the low-wavenumber galaxy component from the power spectrum. These methods circumvent the need for a galaxy model and may have advantages in measuring \overline{m} for galaxies whose structure makes them difficult to fit. We note that the overall approaches of Lorenz *et al.* (1993), Neilsen *et al.* (1997), and Sodemann & Thomsen (1995) in determining \overline{m} is slightly different from the presentation here.

After the mean galaxy profile is removed, the next step is to identify foreground stars, background galaxies, and globular clusters (GCs) in the image. We use a modified version of DOPHOT (Schechter, Mateo, & Saha 1993) to catalogue all objects in the image. Next, we characterize the distribution of these objects in magnitude and radius. This step is very important because the fluctuation amplitude that we measure P_0 includes a *residual* fluctuation signal P_r from *undetected* faint GCs and background galaxies. Ultimately, we want to measure the net fluctuation signal

$$P_{\text{fluc}} = P_0 - P_r. \quad (2)$$

For galaxies at large distances where only the brightest GCs are detectable, P_r swamps P_{fluc} . The SBF technique then becomes a powerful tool for studying the GCs of distant galaxies (Blakeslee & Tonry 1995; Blakeslee *et al.* 1997). To estimate P_r , we assume that the globular cluster luminosity function is Gaussian and that the background galaxy luminosity function is a power law. Fortunately, except when the data are marginal, even a generous error allowance in this step typically contributes only a small amount to the final uncertainty in \overline{m} . As a result, any given measurement of \overline{m} is relatively insensitive to the details of these assumptions.

Next, we determine the total fluctuation amplitude P_0 . After choosing a suitable psf from the galaxy image, we build an expectation power spectrum $E(\vec{k})$ from the psf, the smooth galaxy model, and a mask. (The mask selects the region of the galaxy to be analyzed and excludes GCs, galaxies, and

dust.) The power spectrum of the masked data $P(\vec{k})$ is computed and fitted to the expectation power spectrum such that

$$P(\vec{k}) = P_0 E(\vec{k}) + P_1, \quad (3)$$

where P_1 is a flat “white noise” component. The ratio $(P_0 - P_r)/P_1 = P_{\text{fluc}}/P_1$ is then another good indicator of the signal-to-noise level. Finally, we compute $\overline{m} = -2.5 \log(P_{\text{fluc}}/t) + m_1$.

3. Theoretical Calibrations of the SBF Method

3.1. INITIAL EFFORTS

TAL90 made a pioneering attempt at theoretically calibrating SBF magnitudes. They used the Revised Yale Isochrones (RYI, Green *et al.* 1987) to calculate \overline{M}_V , \overline{M}_R , and \overline{M}_I for model stellar populations covering the conceivable range in metallicity, age, initial mass function, and helium abundance. They also allowed for red or blue horizontal branches and a possible asymptotic giant branch. These RYI-based models indicated that \overline{M}_V and \overline{M}_R were highly sensitive to population age and metallicity, becoming sharply fainter as the population became redder.

However, \overline{M}_I for these models showed very little variation. At the metallicities of elliptical galaxies, it actually became a bit brighter in redder populations. The purely theoretical RYI calibration, quoted here solely for historical purposes, corresponded to: $\overline{M}_I = -1.93 - [(V-I)_0 - 1.15]$. This was a bad calibration; blind acceptance of it would have yielded a Virgo cluster distance of 21 Mpc. However, TAL90 realized that at least the zero point was wrong and so made it fainter by 0.4 mag to be in accord with an assumed distance of 0.7 Mpc for M32. What they were unable to determine from the available data was that the slope of the relation was also in serious error. By purely empirical means, Tonry (1991) found that the correct slope was several times larger and had the opposite sign, with \overline{M}_I fainter in redder populations.

A new edition of the Yale Isochrones, employing much improved model atmosphere flux curves is now available (Demarque *et al.* 1996). These appear to predict fluctuation magnitudes consistent with observations and with the models discussed in the following section (S. Yi 1996, priv. comm.). However, to date no theoretical SBF magnitudes based on these new isochrones have been published.

3.2. THE CURRENT THEORETICAL CALIBRATION

Worthey (1993a, 1994) has produced a realistic set of stellar population models employing some of the best available stellar atmospheric and evo-

lutionary models. He has calculated SBF magnitudes for all the standard optical and near-infrared bandpasses. These calculations (as well as those of Buzzoni 1993) confirm that \overline{M}_I is the most favorable of the optical SBF magnitudes for measuring extragalactic distances.

A fit to the Worthey models over the color range appropriate to elliptical galaxies, $1.05 \lesssim (V-I) \lesssim 1.35$, yields the following theoretical calibration:

$$\overline{M}_I = -1.83 + 4.3 [(V-I)_0 - 1.15], \quad (4)$$

with an rms scatter of 0.10 mag. The models represent homogeneous single-burst stellar populations, but age and metallicity are completely degenerate in their effect here (and changes in the IMF have very little effect). Thus, composite stellar populations will follow this same relation.

Adopting Eq. (4) as a theoretical calibration makes SBF a “secondary” distance indicator, similar to Cepheids. The predicted intrinsic scatter is 0.10 mag or less, depending upon how much variation there is among the stellar populations of elliptical galaxies. We will see in the following section that Eq. (4) agrees with the latest empirical calibration to better than 0.1 mag in zero point.

Buzzoni (1993) has also calculated SBF magnitudes in the optical and near-infrared, comparing them with observations from TAL90 and Tonry (1991). Since his models were on the Johnson system, he transformed the observations using fairly large and uncertain corrections (~ 0.6 mag for \overline{m}_I). Nevertheless, the trend he found between \overline{M}_I and $(V-I)_0$ was consistent with the empirical one and the one predicted by the Worthey models. He derived a distance to M31/M32 consistent with the Cepheid distance.

3.3. STELLAR POPULATIONS ISSUES

A complete discussion of the ramifications of SBF magnitudes and colors for the study of stellar populations is worth a review in its own right. As this article is dedicated to the use of SBF as a distance indicator, we here provide only a cursory treatment of stellar population issues.

TAL90 were the first to consider the effects of age and metallicity on SBF magnitudes, but they were hampered by inadequate models. Worthey (1993a) and Buzzoni (1993) both discussed the effects of stellar population differences on \overline{M} in various bands, arriving at somewhat discordant conclusions. Buzzoni concluded that SBF colors “give so far the more direct and confident evidence of a metal-poor stellar component in [otherwise metal-rich] elliptical galaxies,” while Worthey found “no evidence for composite populations in elliptical galaxies on the basis of fluctuation colors.”

In a separate work, Worthey (1993b) showed how SBF can be a powerful tool in helping to solve the problem of the ultraviolet excess in elliptical

galaxies. He concluded that ultraviolet SBF magnitudes can easily distinguish between the presence of young stars and a hot horizontal branch in a stellar population. His proposal has yet to be applied in practice, however.

Ajhar & Tonry (1994) made the first major observational study of SBF magnitudes as stellar population gauges. They measured $(\bar{m}_V - \bar{m}_I)$ for 19 Galactic globular clusters, clearly showing a correlation of this SBF color with metallicity, due primarily at low metallicity to variation in \bar{M}_V . At the high metallicity end, these authors surmised, \bar{M}_V reaches a minimum brightness near the point where the Mg_2 spectroscopic index saturates ($Mg_2 \sim 0.32$ mag) in giant ellipticals. \bar{M}_I continues to grow fainter, however, causing a large spread of $(\bar{m}_V - \bar{m}_I)$ at a fixed value of Mg_2 .

SBF magnitudes also track stellar population gradients within galaxies. Tonry (1991) showed that the strong radial gradient in \bar{m}_I observed in the dwarf galaxy NGC 205 followed the $(V-I)$ color gradient. However, due to the relatively recent star formation in this galaxy, the \bar{m}_I gradient is actually shallower than would be predicted based on the color gradient (SBF-I). Sodemann and Thomsen (1995, 1996) have found SBF magnitude gradients in accord with theoretical expectations from color gradients in the elliptical galaxies M32 and NGC 3379.

Very little has been published on observations of SBF blueward of the V band. Shopbell *et al.* (1993) reported $(\bar{m}_B - \bar{m}_R) = 2.5 \pm 0.8$ for NGC 5128. Sodemann & Thomsen (1996) have measured \bar{m}_B for M32; their result combined with \bar{m}_R from TAL90 yields $(\bar{m}_B - \bar{m}_R) = 2.42 \pm 0.12$. The Worthey models predict $(\bar{m}_B - \bar{m}_R)$ values in the range of 2.40–2.95 mag for $[Fe/H] \geq -1.5$ and $t \geq 3$ Gyr. We have further, unpublished measurements of this SBF color for M31 and its dE companions and find fair consistency with the models, although the data tend toward the blue side.

Jensen *et al.* (1998a) compare the observed plots of \bar{M}_K vs. integrated $(V-I)_0$ to the predictions from the Worthey models. The models indicate that more luminous, redder elliptical galaxies have both higher metallicities and greater ages. The bluer, more compact ellipticals appear to have both lower mean metallicities and smaller ages, reducing the scatter in \bar{M}_K .

In Figure 1, we construct the observed $(\bar{m}_I - \bar{m}_K)$ vs. $(\bar{m}_V - \bar{m}_I)$ SBF color-color diagram from the available data and compare it to the single-burst model predictions. The comparison indicates that ellipticals generally comprise composite stellar populations. Only the low-luminosity, compact Local Group elliptical M32 and, paradoxically, NGC 4472 and NGC 3379, the brightest ellipticals in Virgo and Leo, respectively, approach the locus of the single-burst population models. Further modeling would be necessary to determine the validity of this result.

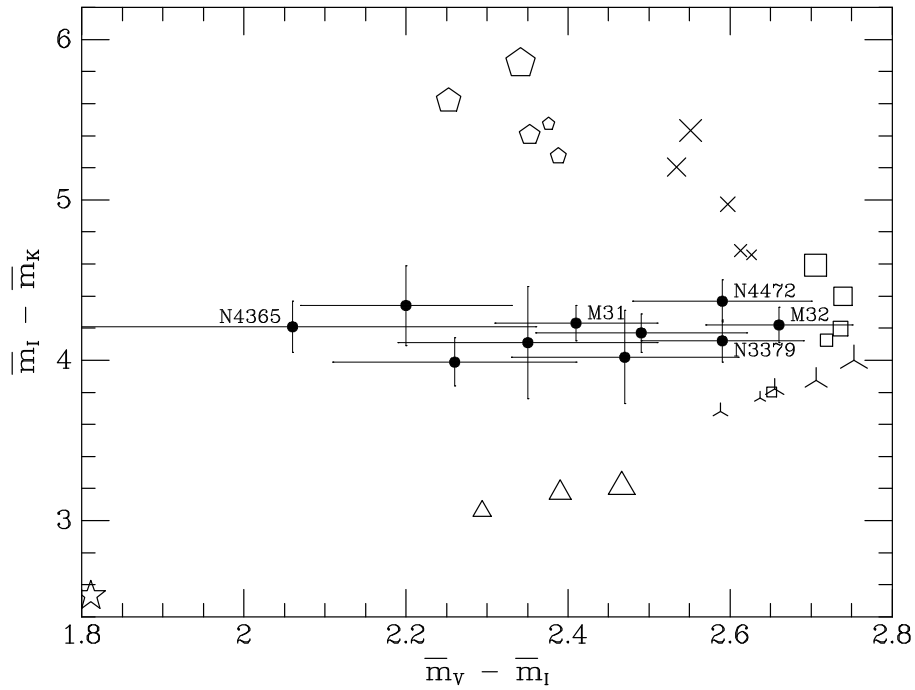


Figure 1. The optical-IR SBF color ($\overline{m}_I - \overline{m}_K$) is plotted against the purely optical ($\overline{m}_V - \overline{m}_I$). Data for 9 ellipticals and the bulge of M31 are shown as filled circles, with several noteworthy galaxies labeled. The V and I data come from TAL90, with a few \overline{m}_I revisions from more recent SBF Survey observations. The \overline{m}_K data are from Luppino & Tonry (1993), Jensen *et al.* (1998a), and Pahre & Mould (1994). Single-burst population models from Worthey (1994) are plotted with the symbols from that work. The models have $[\text{Fe}/\text{H}]$ values of -1.0 (stars), -0.5 (open triangles), -0.25 (skeletal triangles), 0.0 (squares), $+0.25$ (crosses), and $+0.50$ (pentagons) dex. Symbol size is coded according to age: 3, 5, 8, 12, 17 Gyr (the more metal poor models lack the younger ages). Clearly, it is necessary to mix models of various metallicities to reproduce the data.

4. The I-band SBF Distance Survey

Along with Alan Dressler, we have completed a large survey of galaxy distances using the I -band SBF method and are in the process of finalizing the analysis. The first “SBF Survey” paper (SBF-I) details the data sample, observations, and calibration of the survey. The second paper (Tonry *et al.* 1998) will present an analysis of the dynamics of the Virgo supercluster using SBF distances. The third paper (Ajhar *et al.* 1998) will fully describe the theory, data reductions, and analysis methods. A fourth paper (Dressler *et al.* 1998) will analyze the velocity field around the Centaurus cluster and Great Attractor region. Finally, we plan to make the entire imaging data set available to the community.

We have observed over 400 galaxies for the survey, successfully deriving distances to about 340 within a redshift of ~ 4000 km/s. (The rest suffered from inadequate data quality or excessive morphological disturbance or dustiness.) Of the early-type galaxies listed in the Third Reference Catalog of Bright Galaxies (de Vaucouleurs *et al.* 1991), we have observed 75% of those within 1500 km/s and the majority out to 2800 km/s. The sampling is fairly sparse beyond this distance.

4.1. THE EMPIRICAL CALIBRATION

The Survey analysis uses multiple measurements of \overline{m}_I in galaxy groups and clusters to derive empirically the dependence of \overline{M}_I on $(V-I)_0$. SBF-I concluded that the relation is accurately linear over the range of interest (see Figure 2). Extensive comparisons in SBF-I with other distance estimators inspires confidence in the universality of the \overline{M}_I - $(V-I)$ relation. However, an updated comparison between SBF and PNLF distances by Mendez (1998) finds these methods no longer agree to the extent reported by Ciardullo *et al.* (1993).

One difficulty in comparing SBF and Cepheid distances is the fact that Cepheids are young stars residing in late-type galaxies, while the SBF method only works well in the old stellar populations of ellipticals and meaty spiral bulges. We get around this difficulty by using the group distances; the comparison between SBF and Cepheid group distances is especially encouraging and is used to set the zero point of the calibration. The full empirical calibration derived by SBF-I is then:

$$\overline{M}_I = (-1.74 \pm 0.07) + (4.5 \pm 0.25)[(V-I)_0 - 1.15]. \quad (5)$$

This calibration is based on 10 Cepheid and 44 SBF distances in 7 galaxy groups. At the fiducial color of $(V-I)_0 = 1.15$, it is 0.35 mag fainter than the Tonry (1991) calibration. (Although due to the steeper slope, the difference is only ~ 0.2 mag at the very red colors of the Virgo giant ellipticals.) The 1991 zero point estimate relied solely on M31 and M32, and the observational and photometric errors in \overline{m}_I and $(V-I)$ worked coherently in their detrimental affect on that estimate.

Because of the much larger set of calibrating galaxies, and the good agreement between Eq. (5) and the purely theoretical calibration of Eq. (4), we have confidence that the new empirical calibration is a good one. It is possible that Tonry *et al.* (1998) will revise it slightly, according to the final set of SBF Survey measurements, the latest Cepheid distances, and the new Galactic extinction estimates of Schlegel *et al.* (1998), but the changes should be minor.

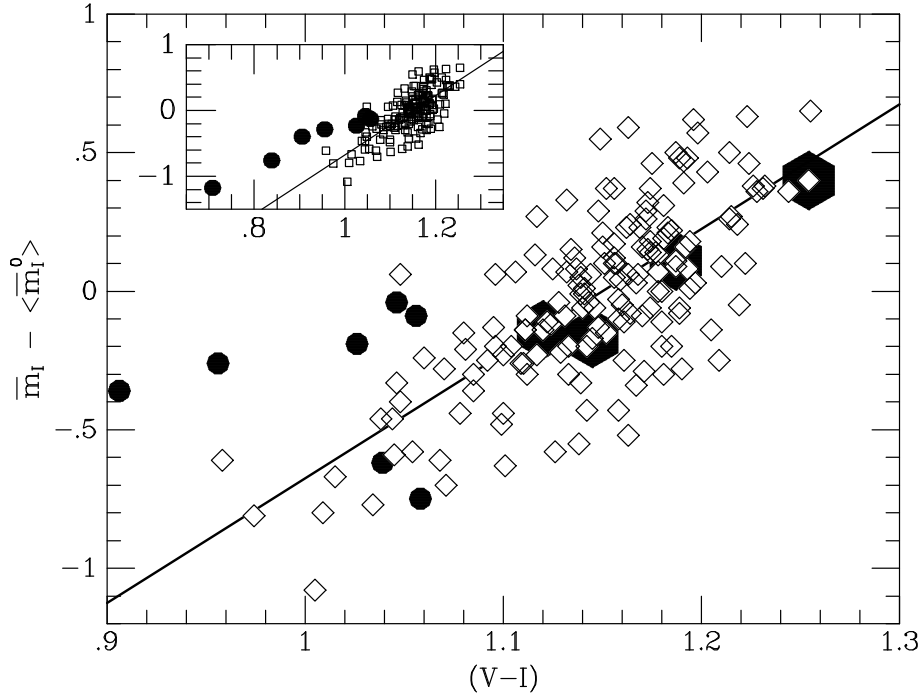


Figure 2. The empirical relation between I -band SBF and $(V-I)_0$ color for all galaxies belonging to the 40 SBF Survey groups. The observables \overline{m}_I and $(V-I)$ are measured for each galaxy; $\langle m_I^0 \rangle$ is the value of \overline{m}_I in each galaxy group at the fiducial color $(V-I)_0 = 1.15$. The line represents a simultaneous fit to the forty values of $\langle m_I^0 \rangle$ along with a universal slope for the dependence of $(\overline{m}_I - \langle m_I^0 \rangle)$ on $(V-I)_0$. Four spiral galaxies with Cepheid and SBF distances are plotted as large, solid hexagons, demonstrating that SBF is the same for spiral bulges as for elliptical and S0 galaxies. The round, solid points above the line are various locations in NGC 205, and those below the line are NGC 147 and NGC 185; none of these Local Group dwarfs were used in the fit. The inset shows the locations of NGC 5253 and IC 4182, placed according to their Cepheid distances. These galaxies and NGC 205 deviate from the relation because their young blue stars change the overall galaxy color by a large amount but are not very luminous in the I band compared to the stars at the top of the RGB, the main contributors to \overline{m}_I .

4.2. THE GREATER HUBBLE FLOW AND H_0

The SBF Survey can be tied to the Hubble flow via comparison with other distance estimators extending to larger redshift. Tying to large redshift using the $D_n - \sigma$ distances of Faber *et al.* (1989) or the “Mark II” Tully-Fisher distances (both in km/s), SBF-I found values of the Hubble constant near $H_0 \sim 86$ km/s/Mpc. In contrast, the tie to large redshift via Type Ia supernova (Hamuy *et al.* 1995) yielded $H_0 \sim 72$ km/s/Mpc. After some discussion, SBF-I saw no reason to exclude either large-redshift tie, and so

offered 72–86 km/s/Mpc as the likely range of H_0 .

It is difficult to constrain H_0 directly from ground-based optical SBF measurements. Tonry *et al.* (1998) address this problem in the context of Virgo infall. Section 6 reviews H_0 determinations from SBF measurements using *HST*. Direct constraints on H_0 from the ground-based near-infrared SBF measurements of Jensen *et al.* (1998b) are given in Section 8.

5. Other Ground-based Optical SBF Distances

Several other groups have published optical SBF distances from ground-based data. The first of these was Lorenz *et al.* (1993) who showed that the S0 galaxy NGC 1375 lay within the Fornax cluster. Tonry (1991) had derived a surprisingly bright \overline{m}_I for this galaxy, placing it about 3 Mpc in front of the rest of the cluster. He suggested that the SBF measurement was corrupted by the isophotal distortions. Lorenz *et al.* were more meticulous in restricting their analysis to the bulge, avoiding the “strong disk and ring-like structure seen in absorption.” For the neighboring elliptical NGC 1374, these authors obtained a distance in agreement with Tonry (1991). In addition, the \overline{m}_I measurements for M32 and NGC 3379 by Sodemann & Thomsen (1995, 1996) agree closely with those of TAL90.

A novel approach was taken by Shopbell *et al.* (1993), who measured SBF from digitized wide-field photographic plates of NGC 5128 (Cen A). They obtained a distance in close agreement with the one reported by Tonry & Schechter (1990) using the “traditional” CCD approach. Shopbell *et al.* demonstrated that, remarkably, the method could have been applied long ago, before the development of CCDs. However, due to the large amount of grain noise from the photographic emulsion, it would likely work for only the nearest ellipticals with strong SBF signals.

Simard & Pritchett (1994) published distances to two Coma I group galaxies from *V*-band SBF measurements. They found a distance of 15 Mpc for the elliptical NGC 4494 but only 10 Mpc for the edge-on spiral NGC 4565, concluding it was in the foreground. We have *I*-band measurements from the SBF Survey that place both galaxies at 16 Mpc.

We are wary of *V*-band SBF because it has not been well characterized observationally. Buzzoni (1993) discusses at length the acute sensitivity of \overline{M}_V to metallicity and age in his models. However, Worthey’s (1993) models indicate that \overline{M}_V is nearly as well-behaved as \overline{M}_I . In either case, it should be noted that the bulge of NGC 4565 has an integrated color similar to that of NGC 4494. However, being so faint, the *V*-band fluctuations are difficult to detect at ~ 15 Mpc, except in giant ellipticals with ample surface area for measuring the signal. It would be easy to mistake morphological distortions associated with the disk for true SBF.

Ajhar & Tonry (1994) published SBF distances to their 19 Galactic globular clusters, deriving the value of \overline{M}_I from RR Lyrae distances. Ajhar *et al.* (1996) used that calibration along with *HST* data on an M31 globular to obtain $(m-M) = 24.56 \pm 0.12$, in agreement with Cepheids. Finally, we note that Tiede *et al.* (1995) calculated \overline{m}_V and \overline{m}_I for the Galactic bulge from deep star counts through Baade’s window. Their results give a Galactic center distance of 10 ± 2 kpc with the SBF-I calibration; most of the uncertainty is due to an uncertain $(V-I)_0$ for the bulge.

6. Ground-based SBF Measurements in the Near-Infrared

SBF magnitudes are much brighter in the near-infrared (IR) for early-type galaxies, with $(\overline{m}_I - \overline{m}_K) > 4.0$. It therefore seems natural for the method to transit into the IR as the detectors improve, *if* SBF magnitudes behave predictably there. Several studies of IR SBF have already been done, and the promise held by this method has begun to reach fruition with the thesis work of J. Jensen. Before surveying the observations, we briefly examine the model predictions.

6.1. PREDICTED BEHAVIOR OF IR SBF MAGNITUDES

Somewhere between I and J , the sense of the \overline{M} -color relationship reverses, according to the models of Worthey (1993a). Redder model populations therefore have brighter JHK SBF magnitudes, but the predicted trends are weak, *e.g.*: $\overline{M}_K \sim -1.2(V-I) - 4.2$ [compare Eq. (4)]. On the other hand, the Buzzoni (1993) models still show a decline in brightness with color for \overline{M}_K , and are fainter by ~ 0.6 mag in the mean. Pahre & Mould (1994) found better agreement with the Worthey models and suggested the difference was due to Worthey’s inclusion of an empirical M-giant population.

Although the predicted changes in \overline{M}_K are relatively small, variations in metallicity and age are no longer degenerate in their effects, whereas they are for \overline{M}_I . Age differences therefore induce scatter in the model \overline{M}_K -metallicity relation. For this reason, it was initially unclear whether or not \overline{M}_K would be a reliable distance indicator. Ironically, it has proven to be a near perfect one, as the following section recounts.

6.2. OBSERVATIONS OF IR SBF

Luppino & Tonry (1993) used a 256^2 NICMOS3 array and a K' filter ($\lambda_C = 2.1 \mu\text{m}$) to measure \overline{m}_K in M31, M32, and Maffei 1, a heavily reddened elliptical lying close to the Galactic plane. Adopting the Cepheid distance of 0.77 Mpc (Freedman & Madore 1990), they found $\overline{M}_K = -5.61 \pm 0.14$ for the bulge of M31 and $\overline{M}_K = -5.87 \pm 0.14$ for M32. Taking the M31 result

as a calibration, they derived a distance of 4.2 ± 0.5 Mpc to Maffei 1. They concluded that Maffei 1 is a true giant elliptical, clearly not a Local Group member as Spinrad *et al.* (1971) suggested, and twice as distant as the Faber-Jackson estimate of Buta & McCall (1983). The 0.26 mag difference in \overline{M}_K between M31 and M32 was troubling, and they speculated that it might be due to an extended AGB in M32. Using M32 as the calibrator would only have increased the Maffei 1 distance to 4.7 Mpc, however.

Pahre & Mould (1994) also used a NICMOS3 array but a “K-short” filter ($\lambda_C = 2.16 \mu\text{m}$) to measure \overline{m}_K for NGC 3379 and 8 Virgo ellipticals. Excluding two apparent outliers, they derived $\langle \overline{M}_K \rangle = -5.74$; the rms dispersion of 0.20 mag was comparable to their typical measurement error of 0.18 mag. They modeled the effects of a hypothetical extended AGB on \overline{M}_K and concluded that such a component must not be common in giant ellipticals. Their measurement for NGC 4365 indicated that it was in the Virgo cluster proper, not in the background W Cloud as TAL90 had found (but see below).

Jensen *et al.* (1996) measured \overline{m}_K for 7 Virgo ellipticals and the bulge of M31 using the same instrument and filter as Luppino & Tonry (1993). Combining their results with those from Pahre & Mould (1994), they discovered a bias affecting the low signal-to-noise (S/N) measurements and attributed it to errors in sky subtraction and variations in the dark current on scales comparable to the psf. They conservatively concluded that $S/N \sim P_0/P_1 \gtrsim 4$ was required for accurate SBF measurements with present IR arrays. Accounting for the bias, they found $\langle \overline{M}_K \rangle \approx -5.62$, with an rms dispersion of 0.29 mag, similar to the measurement errors.

More recently, Jensen *et al.* (1998a) have used the large format 1024² QUIRC near-IR camera to measure \overline{m}_K for 5 galaxies in the Fornax cluster, 4 in the Eridanus group and NGC 4365. They made several improvements to the analysis techniques, including the use of optical images to identify and remove globular clusters and background galaxies from the IR images. The improved methodology was also used to reanalyze the earlier Virgo data. The new high-S/N observation of NGC 4365 clearly showed that this galaxy lies about 0.65 mag behind the Virgo core towards the W Cloud, in precise agreement with the *I*-band distance.

Calibrating the *K*-band SBF measurements with 5 Cepheid distances, Jensen *et al.* (1998a) derived $\langle \overline{M}_K \rangle = -5.61 \pm 0.06$ for a sample of 11 galaxies with high-S/N data. This is within the range of the Worthey (1993a) models. There is an additional systematic uncertainty of ~ 0.1 mag from the zero-point of the Cepheid scale. No significant change in \overline{M}_K was detected as a function of color or metallicity. If the models are accepted at face value, the constancy of \overline{M}_K implies that bluer, less luminous ellipticals are younger than their giant kindred. In addition, anomalous AGB popu-

lations must be rare or absent, though could contribute marginally to \overline{M}_K in a couple 2σ outliers, including M32. \overline{M}_K is thus an excellent standard candle without need of color correction.

Jensen *et al.* (1998b) have pushed their ground-based K -band method further, measuring distances to NGC 4889 in the Coma cluster ($cz = 7186$ km/s) and NGC 3309/NGC 3311 in the Hydra cluster ($cz = 4054$ km/s). Their Coma distance translates to $H_0 = 85 \pm 11$ km/s/Mpc, and their distance of 46 ± 5 Mpc for Hydra implies a small radial peculiar velocity for this cluster, $v_p \lesssim 400$ km/s. This is consistent with the Great Attractor model of Lynden-Bell *et al.* (1988), which places Hydra at a right angle to the G.A., with the resultant motion perpendicular to our line of sight.

The great success of the IR SBF method so far strongly suggests that it can be pushed even further, and attain higher accuracy, with the larger telescopes and better IR detectors now coming on-line. Yet, because of the dramatically lower background, the promise of the method is far greater with space-based observations, as we discuss in the following section.

7. SBF Distances from the Hubble Space Telescope

7.1. MINING THE ARCHIVE

A number of galaxy observations taken for other programs have been used for SBF measurements. Ajhar *et al.* (1997) have calibrated the SBF technique with WFPC2 in the F814W filter, which approximates the Kron-Cousins I band. They measured \overline{m}_{814W} for 16 galaxies and compared their results to \overline{m}_I measurements from the ground. The sample derives from a GTO program to study the cores of early-type galaxies, but the integration times were sufficient for measuring SBF amplitudes.

As discussed in Section 3.3, SBF magnitudes depend strongly on wavelength. For instance, an elliptical with $(R-I) = 0.6$ might have $(\overline{m}_R - \overline{m}_I) = 1.5$. As the total WFPC2/F814W bandpass is wider and extends a bit to the blue of I_{KC} , an independent calibration was deemed necessary. Ajhar *et al.* concluded that $\overline{M}_{814W} \approx \overline{M}_I$ for $(V-I) \approx 1.15$, but the slope of the color dependence was steeper at the 2.7σ level. The best-fit value for the slope was 6.5. The distances obtained with this calibration agreed well with those from the SBF Survey.

Several other authors have measured SBF distances with *HST*. Neilson *et al.* (1997) used WFPC2 observations taken in parallel mode to measure a distance of 15.6 ± 1.0 Mpc for the Virgo galaxy NGC 4478. Thomsen *et al.* (1997) have pushed the limits of the technique in an effort to measure the distance to the Coma cluster elliptical NGC 4881. The WFPC2 image of this galaxy was taken for a study of its globular cluster system and yielded a signal of only $0.7 e^-/\overline{m}$ (*cf.* Section 2). They employed a calibration based

on Mg_2 index and arrived at a Coma cluster distance of 102 ± 14 Mpc, implying $H_0 = 71 \pm 11$ km/s/Mpc.

Morris & Shanks (1998) measured SBF magnitudes using 3 of the 16 WFPC2 galaxy observations in the Ajhar *et al.* (1997) sample. Applying very different methods for galaxy subtraction, psf-fitting, and background correction, they obtained reassuringly similar values of \overline{m}_{814W} (a median difference of 0.11 mag). These authors interpreted their results somewhat differently, however; we discuss their conclusions further in Section 8.1.

7.2. SBF PROGRAMS WITH *HST*

Prior to refurbishment, *HST* was not useful for SBF measurements. Since then, however, SBF observations have been allocated time during Cycles 5 (“The Far Field Hubble Constant”) and 6 (“The Cosmic Velocity of the Great Attractor”) using WFPC2, and Cycle 7 using NICMOS (“The SBF Hubble Diagram”). We discuss each of these proposals, and a GTO SBF study by Pahre *et al.* (1998), below.

The Cycle 5 observations were successful in providing distances to four Abell clusters and in calibrating the zero point of the brightest cluster galaxy distance scale (Lauer *et al.* 1998). This program yielded a value of H_0 dependent on the Cepheid distance scale on the near end and the linearity of the Hubble flow to 4500 km/s at the far end. Another goal was to test the validity of three reference frames: the CMB frame, the Local Group frame (perhaps modified by Virgo infall), and the “Abell Cluster Inertial” frame proposed by Lauer and Postman. The agreement between SBF distance and velocity was excellent in the CMB frame ($\chi^2/N = 0.3$) and poor in the ACI frame ($\chi^2/N = 2.4$).

Pahre *et al.* (1998) have used WFPC2 IDT/GTO observations to measure the distance to NGC 4373, a large elliptical in its own group within the Hydra-Centaurus supercluster. Adopting the calibration of Ajhar *et al.* (1997), they find $d = 39.6 \pm 2.2$ Mpc for this galaxy and derive a peculiar velocity of 415 ± 300 km/s. This peculiar velocity is about half as large as the 838 km/s prediction from the Great Attractor model proposed by Lynden-Bell *et al.* (1988) based on $D_n - \sigma$ measurements.

The Cycle 6 SBF program explores this issue further, probing the size of the Great Attractor by measuring SBF distances (and peculiar velocities) to two galaxies in the Centaurus cluster, two galaxies at 5000 km/s judged to be on the far side of the G.A. (and hence should reveal backside infall), and one galaxy of comparable distance at an angle where the peculiar velocity should be negligible. Because of the NICMOS cryogen problem, the observations for this program are not yet complete, but the data taken so far appear excellent. We expect them to provide definitive answers to the

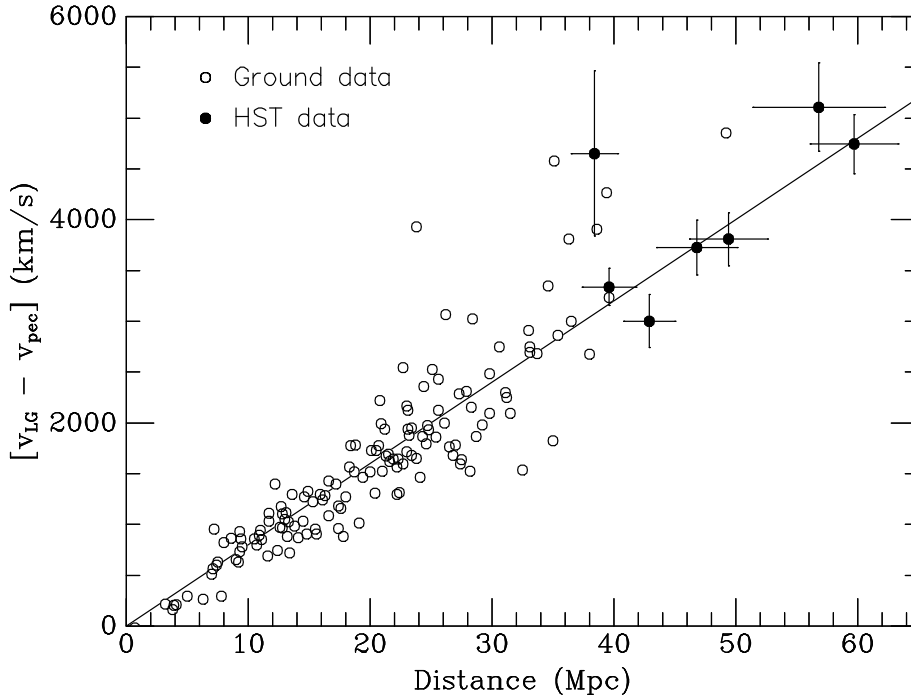


Figure 3. The I -band SBF Hubble diagram. SBF distances measured with WFPC2 on *HST* are shown as filled symbols; distances from the ground-based SBF Survey are shown as open symbols, with error bars omitted for clarity. The velocities are in the Local Group frame, corrected for a nonlinear Virgo infall model of amplitude 200 km/s at the Local Group (Tonry *et al.* 1998). The very discrepant *HST* point near 39 Mpc is a high peculiar velocity galaxy in the “Cen-45” cluster.

questions of where the Centaurus/G.A. flow comes to rest with respect to the CMB, and what the precise amplitude of the flow is. Figure 3 displays the SBF Hubble diagram for the Cycles 5 and 6 data, combined with the ground-based I -band Survey data.

SBF is about 30 times brighter in the H -band than in the I -band, and NICMOS affords an enormous advantage over ground-based IR observations because its sky background is at least 100 times fainter. The Cycle 7 program seeks to calibrate SBF in the F160W filter (similar to H) and then measure H_0 at three different distances: 4500 km/s, 7000 km/s, and 10,000 km/s. The project has collected data on a “calibrator” sample consisting of 10 nearby galaxies in clusters where good Cepheid distances exist (Leo I, Virgo, and Fornax). These galaxies were chosen to span a range of color and luminosity that will allow the dependence of F160W SBF on metallicity and age to be characterized.

The “nearby” sample at 4500 km/s consists of 5 galaxies for which there are WFPC2 observations, making it possible to directly tie together the SBF distances measured by the two instruments. Along with the calibrators, these should yield a Hubble constant valid within about 4500 km/s. The “intermediate” sample comprises 6 central galaxies in Abell clusters in the redshift range 5500–9500 km/s. These clusters were selected to be at the vertices of an octahedron which symmetrically straddles the Galactic plane. We thus expect that the mean H_0 derived from this data set will be extremely insensitive to the velocity reference frame adopted. Moreover, we will obtain a good estimate of the reference frame in which these galaxies are at rest. Finally, the “distant” sample was trimmed to a single cluster at 10,000 km/s. Most of the data for this project have been taken, and the first pass reductions are extremely promising.

8. Evaluating SBF as a Distance Indicator

8.1. ADDRESSING SOME CRITICISMS

One of the primary points of contention surrounding the SBF method is its calibration. The present calibration from SBF-I still may not be perfect. Systematic errors of ~ 0.1 mag could remain, but we have noted reasons for believing that the zero-point error is not much larger than this. Moreover, earlier indications of residual correlations between inferred SBF distance and galaxy luminosity (Tonry *et al.* 1989), integrated color (Tonry *et al.* 1990), and Mg_2 index (Lorenz *et al.* 1993; Tammann 1992) vanish in the light of the new \overline{M}_I –($V-I$) calibration (SBF-I).

Recently, Morris & Shanks (1998, hereafter MS98) have suggested that the lower limit for errors in I -band SBF distances is actually 0.17 mag, based on their reductions of three galaxy observations in the *HST* archive. Much of this conclusion appears to stem from the 0.05 mag uncertainties they derived for their ($V-I$) values. If ($V-I$)₀ is known to only 0.05 mag, then the minimum SBF distance error is actually 0.23 mag, due to the $4.5(V-I)_0$ term in the \overline{M}_I calibration. For this reason, SBF-I expended much effort to ensure accurate and uniform photometry to better than 0.02 mag in ($V-I$) for the SBF Survey (see 8.3.4 below).

All three of the *HST* observations analyzed by MS98 were included in the sample of 16 galaxies from Ajhar *et al.* (1997). Unlike MS98, Ajhar *et al.* did not attempt to analyze data from the WF cameras, which badly under-sample the psf. Comparing just the MS98 PC chip measurements from their Table 8 to Ajhar *et al.* gives differences of $+0.21 \pm 0.11$ mag for NGC 3379, -0.11 ± 0.08 mag for NGC 4406, and -0.07 ± 0.11 mag for NGC 4472. The agreement in \overline{m} itself is reasonable; only the NGC 3379 results differ by nearly 2σ . Pahre *et al.* (1998) also measured \overline{m} for the same NGC 3379

and NGC 4406 *HST* data in order to test their SBF analysis method on the marginally sampled PC images. Compared to the \overline{m} values of Pahre *et al.*, those of MS98 differ by +0.36 mag for NGC 3379 and +0.04 mag for NGC 4406. Both Ajhar *et al.* and Pahre *et al.* found results for NGC 3379 consistent with the ground-based numbers from the SBF survey.

The MS98 measurement for NGC 3379 is thus inconsistent with both the Ajhar *et al.* and Pahre *et al.* *HST* results, and with the ground-based results from the SBF Survey and Sodemann & Thomsen (1996). One cannot conclude from this single discrepancy, or from $(V-I)$ measurements with 0.05 mag uncertainties, that the average distance error in the hundreds of ground-based SBF distances is 0.25 mag and that the minimum error is 0.17 mag. We refer the reader to SBF-I for an extensive statistical analysis of the ground-based SBF distance errors.

8.2. “COSMIC” SCATTER

We rehash here the evidence for universality in the behavior of the two main SBF magnitudes utilized for estimating galaxy distances.

Based on SBF and color measurements for ~ 150 galaxies in ~ 40 nearby galaxy groups, SBF-I concluded that the quantity $\overline{M}_I - 4.5 [(V-I)_0 - 1.15]$ is a standard candle among early-type galaxies in the color range $1.0 < (V-I)_0 < 1.3$. Calibration via Cepheids yielded an absolute magnitude of -1.74 mag for this standard candle. From an analysis of χ^2 , they concluded that the intrinsic, or “cosmic,” scatter was less than 0.1 mag; most likely it was ~ 0.05 mag. The stellar population models of Worthey (1993) indicate that the above $\overline{M}_I - (V-I)_0$ relation is a standard candle with intrinsic scatter < 0.11 mag, depending upon the amount of variation present among the stellar populations of elliptical galaxies. These models give a calibration brighter by ~ 0.08 mag than the empirical one.

The second most commonly utilized SBF magnitude for distance estimation is \overline{m}_K . The observations by Jensen *et al.* (1998a) indicate that \overline{M}_K is by itself a standard candle with a cosmic scatter of only 0.06 mag for early-type galaxies in the limited color range $1.15 < (V-I)_0 < 1.27$. The models predict that \overline{M}_K should systematically brighten by ~ 0.15 mag even over this color range, if all ellipticals are coeval. Thus, if both the models and the observations are correct, there must be an age-metallicity conspiracy among early-type galaxies to keep \overline{M}_K constant. Further investigation along both lines is needed to test the significance of this result.

8.3. WHAT CAN GO WRONG

If SBF is such a great standard candle, why might some distances be wrong? Below, we list possible problems that can affect distance estimates.

8.3.1. *Difficult Galaxies*

There have been some clear discrepancies with SBF distances involving measurements on non-ideal galaxies, such as the edge-on spiral NGC 4565 (Simard & Pritchett 1994, as compared to the SBF Survey) and the disk S0 NGC 1375 (Tonry 1991, compared to Lorenz *et al.* 1993). For these two cases it appears that the better measurement gives the correct distance. Thus, the problems were with the reductions, not due to intrinsic difference in SBF magnitude between spiral bulges and ellipticals. It pays to take pains. With well over 300 SBF distances in the Survey, it is difficult to ensure a uniform pain threshold for all the reductions; there may be a few bad distances in the complete data set for this reason.

Unfortunately, Cepheids only dwell in the most difficult galaxies for SBF. A case in point is the flocculent spiral NGC 7331, for which we attempted to measure an SBF distance from its smooth outer disk. SBF-I reported 12 Mpc for this galaxy in anticipation of the Cepheid distance, which comes in at 15 ± 1 Mpc (S. Hughes 1998, priv. comm.). We reanalyzed the data, but they gave the same \overline{m}_I . Although the outer disk appears smooth, the stars within it must be correlated on the scale at which the SBF was measured, ~ 22 pc at this distance; if this is the case, the SBF method will not work. Fortunately, this is not a problem for ellipticals and other “hot” stellar systems. It thus appears we were over-zealous in our attempt to measure SBF distances for every possible Cepheid-bearing galaxy.

A similar problem may affect the SBF distance for the edge-on disk galaxy NGC 3115. The PNLF and RGB tip methods give 10.9 ± 0.7 Mpc (Elson 1997), while the SBF distance is 9.2 ± 0.5 Mpc. Remeasurement of \overline{m} from Elson’s *HST* data in a clean region of the bulge well away from the disk would help in understanding the discrepancy for this galaxy.

8.3.2. *PSF Mismatch*

An accurate SBF amplitude depends on having a good star to serve as a psf template. This is usually not a problem, but occasionally for a galaxy at high galactic latitude, the pickings get rather slim. As all power spectrum measurements are referenced to the psf template power spectrum, an error of 5% in its normalization translates into a 0.05 mag error in \overline{m} . This is a bigger problem in the IR, where psf stars must contend with an extremely bright sky (see Jensen *et al.* 1996). For *HST* images, one has recourse to a synthetic psf, although most groups opt for empirical ones if at all possible (e.g., Ajhar *et al.* 1997; Pahre *et al.* 1998; Lauer *et al.* 1998).

8.3.3. *Bad Background Luminosity Function Model*

The ability to detect, remove, and model the faint globular clusters and background sources so that P_0 is dominated by the SBF and not by the

background variance P_r , and so that P_r can be accurately estimated, is the limiting factor in the ground-based I -band SBF method. Greatly improved background source removal due to superior resolution is the big advantage *HST* holds for the optical SBF method. (The major advantage of *HST* in the IR is the much lower background.)

Faint point source removal and luminosity function modeling for estimating P_r are discussed in detail by Tonry & Schneider (1988), TAL90, and Ajhar *et al.* (1998), to which we refer the reader. One thing worth noting here is that the uncertainty estimate for P_r should not be made directly proportional to the P_r estimate. Otherwise, if the estimated P_r is less than the true residual variance, the P_r uncertainty will be underestimated by the same factor, making the derived \bar{m} simultaneously too bright and overly significant. This is avoided by estimating the uncertainty in P_r from the depth of the point source removal (see Ajhar *et al.* 1998).

8.3.4. *Good \bar{m}_I , Bad $(V-I)$*

With all the trouble involved in measuring \bar{m}_I , one might think something as simple as the galaxy color would be easy. This is a dangerous trap. Since $\bar{M}_I \sim 4.5(V-I)$, the $(V-I)_0$ color must be known to 0.024 mag for an accuracy of 5% in distance. SBF-I described an entire secondary survey undertaken on the McGraw-Hill 1.3 m telescope to help ensure adequate $(V-I)$ surface photometry for the primary SBF Survey.

If a color gradient is present in a galaxy, care must be taken to calculate \bar{M}_I using the $(V-I)_0$ color determined from the region over which \bar{m}_I was measured. There are bulge/disk concerns here, too. Galaxy disks are usually bluer than their bulges; if \bar{m}_I is measured in the bulge, then the disk must be entirely removed before measuring $(V-I)$, or the \bar{M}_I estimate will be too bright. Of course, if dust contaminates the color measurement, the \bar{M}_I estimate will be too faint. (SBF-I discuss these issues further.)

8.3.5. *Bad Extinction Estimate*

Finally, even if one is careful about photometry and color gradients, an inaccurate extinction estimate will produce a bad distance. Because of the way $(V-I)_0$ comes into the calculation of \bar{M}_I , underestimating the Galactic extinction actually yields a *smaller* distance, as the effect of making \bar{m}_I artificially dim is overwhelmed by the effect of making $(V-I)_0$ too red. The error introduced into the distance modulus from an error δA_B in the B -band extinction is: $\delta(\bar{M}_I - \bar{m}_I) \approx +0.83 \delta A_B$. SBF-I used Burstein & Heiles (1984) extinctions; in the next paper we will convert to the Schlegel *et al.* (1998) extinctions determined from 100 μm dust emission.

9. The Future of SBF

To push much further with optical SBF distances from the ground will require adaptive optics techniques to deliver images with seeing consistently $\lesssim 0''.45$ FWHM. This may soon be a reality, but the combination of the $0''.1$ psf and a sky darker by orders of magnitude places the real future of SBF observations in space.

It seems likely to us that further application of the optical SBF method from space will eventually map out the pattern of galaxy and cluster velocity flows to distances at which the motions become just a few percent of the Hubble velocity. There is no other method for measuring elliptical galaxy distances that can compare for completeness, depth, and accuracy.

Before this can be accomplished, the slope of the SBF calibration in the F814W filter must be verified directly from multiple measurements of galaxies in tight groups and clusters. This will avoid compounding errors from individual ground-based distances. With recent F814W observations of several ellipticals in Fornax, there is now enough data in the *HST* archive to do this, and so we expect to have a final calibration soon.

With SBF being so much brighter and so well-behaved in the near-IR, and the gain in terms of a darker background being so immense, IR SBF from space may be the most promising method of all. Although most of this review has been concerned with optical measurements, it is possible that a similar review in another decade will deal almost exclusively with IR SBF measurements. Again, there needs to be more done to ensure accurate calibrations of \overline{M}_K and \overline{M}_H .

Finally, there is need for improved models, and will remain such need until we fully understand the behavior of \overline{M} across the spectrum. The SBF method will then be independent of the Cepheid calibration. Moreover, we will have an excellent handle on the age and metallicity mixtures in elliptical galaxies, and how these mixtures change with luminosity and other galaxy properties.

References

- Ajhar, E.A., Grillmair, C.J., Lauer, T.R., Baum, W.A., Faber, S.M., Holtzman, J.A., Lynds, C.R., & O'Neil, E.J., Jr. 1996, *Astron. J.*, **111**, 1110.
- Ajhar, E.A., Lauer, T.R., Tonry, J.L., Blakeslee, J.P., Dressler, A., Holtzman, J.A., Postman, M. 1997, *Astron. J.*, **114**, 626.
- Ajhar, E.A. & Tonry, J.L. 1994, *Ap. J.*, **429**, 557.
- Ajhar, E.A., Tonry, J.L., Blakeslee, J.P., & Dressler, A. 1998, in preparation.
- Blakeslee, J.P. & Tonry, J.L. 1995, *Ap. J.*, **442**, 579.
- Blakeslee, J.P., Tonry, J.L., & Metzger, M.R. 1997, *Astron. J.*, **114**, 482.
- Burstein, D., & Heiles, C. 1984, *Ap. J. Suppl.*, **54**, 33.
- Buta, R.J. & McCall, M.L. 1983, *MNRAS*, **205**, 131.
- Buzzoni, A. 1993, *Astron. Astrophys.*, **275**, 433.

- Ciardullo, R., Jacoby, G.H. & Tonry, J.L. 1993, *Ap. J.*, **419**, 479.
- Demarque, P., Chaboyer, B., Guenther, D., Pinsonneault, L., Pinsonneault, M., & Yi, S. 1996, *The Yale Isochrones 1996* (<http://shemesh.gsfc.nasa.gov/astronomy.html>).
- de Vaucouleurs, G., de Vaucouleurs, A., Corwin, H.G., Jr., Buta, R.J., Paturel, G., & Fouqué, P. 1991, *Third Reference Catalog of Bright Galaxies* (New York: Springer).
- Dressler, A., Tonry, J.L., Ajhar, E.A., & Blakeslee, J.P. 1998, in preparation.
- Elson, R.A.W. 1997 *MNRAS*, **286**, 771.
- Faber, S.M., Wegner, G., Burstein, D., Davies, R.L., Dressler, A., Lynden-Bell, D., & Terlevich, R.J. 1989, *Ap. J. Suppl.*, **69**, 763.
- Freedman, W.L. & Madore, B.F. 1990, *Ap. J.*, **365**, 186.
- Green, E.M., Demarque, P., & King, C.R. 1987, *The Revised Yale Isochrones and Luminosity Functions*, (New Haven: Yale).
- Hamuy, M., Phillips, M.M., Maza, J., Suntzeff, N.B., Schommer, R.A., & Aviles, R. 1995, *Astron. J.*, **109**, 1.
- Jacoby, G.H., Branch, D., Ciardullo, R., Davies, R.L., Harris, W.E., Pierce, M.J., Pritchett, C.J., Tonry, J.L., Welch D.L. 1992, *Publ. Astron. Soc. Pac.*, **104**, 599.
- Jensen, J.B., Luppino, G.A., & Tonry, J.L. 1996, *Ap. J.*, **468**, 519.
- Jensen, J.B., Tonry, J.L., & Luppino, G.A. 1998a, *Ap. J.*, in press.
- Jensen, J.B., Tonry, J.L., & Luppino, G.A. 1998b, *Ap. J.*, submitted.
- Lauer, T.R., Tonry, J.L., Postman, M., Ajhar, E.A., Holtzman, J. A., 1998, *Astron. J.*, **499**, 577.
- Lorenz, H., Böhm, P., Capaccioli, M., Richter, G.M., & Longo, G. 1993, *Astron. Astrophys. Lett.*, **277**, L15.
- Luppino, G.A. & Tonry, J.L. 1993, *Ap. J.*, **410**, 81.
- Lynden-Bell, D., Faber, S.M., Burstein, D., Davies, R.L., Dressler, A., Terlevich, R.J., & Wegner, G. 1988, *Ap. J.*, **326**, 19.
- Morris, P.W. & Shanks T. 1998, *MNRAS*, submitted (MS98).
- Neilsen, E.H., Jr., Tsvetanov, Z.I., & Ford, H.C. 1997, *Ap. J.*, **483**, 745.
- Mendez, R.H. 1998, this volume.
- Pahre, M. A., *et al.* 1998, *Ap. J.*, in press.
- Pahre, M. A. & Mould, J. R. 1994, *Ap. J.*, **433**, 567.
- Schechter, P.L., Mateo, M. & Saha, A. 1993, *Publ. Astron. Soc. Pac.*, **105**, 1342.
- Schlegel, D.J., Finkbeiner, D.P., & Davis, M. 1998, *Ap. J.*, **500**, 525.
- Shoppell, P.L., Bland-Hawthorn, J., & Malin, D. F. 1993, *Astron. J.*, **106**, 1344.
- Simard, L. & Pritchett, C.J. 1994, *Ap. J.*, **107**, 503.
- Sodemann, M. & Thomsen, B. 1995, *Astron. J.*, **110**, 179.
- Sodemann, M. & Thomsen, B. 1996, *Astron. J.*, **111**, 208.
- Spinrad, H., Sargent, W.L.W., Oke, J.B., Neugebauer, G., Landau, R., King, I.R., Gunn, J.E., Garmire, G., Dieter, N.H. 1971, *Ap. J.*, **163**, L25.
- Tammann, G.A. 1992, *Physica Scripta*, **T43**, 31.
- Thomsen, B., Baum, W.A., Hammergren, M., & Worthey, G. 1997, *Ap. J. Lett.*, **483**, L37.
- Tiede, G.P., Frogel, J.A., & Terndrup, D.M. 1995, *Astron. J.*, **110**, 2788.
- Tonry, J.L. 1991, *Ap. J. Lett.*, **373**, L1.
- Tonry, J.L. 1996, in *The Extragalactic Distance Scale*, eds. M. Livio, M. Donahue, & N. Panagia (Cambridge: Cambridge Univ. Press), 297.
- Tonry, J.L., Ajhar, E.A., & Luppino, G.A. 1989, *Ap. J. Lett.*, **346**, L57.
- Tonry, J.L., Ajhar, E.A., & Luppino, G.A. 1990, *Astron. J.*, **100**, 1416 (TAL90).
- Tonry, J.L., Blakeslee, J.P., Ajhar, E.A., & Dressler, A. 1997, *Ap. J.*, **475**, 399 (SBF-I).
- Tonry, J.L., Blakeslee, J.P., Ajhar, E.A., & Dressler, A. 1998, in preparation.
- Tonry, J.L. & Schechter, P.L. 1990, *Astron. J.*, **100**, 1794.
- Tonry, J.L. & Schneider, D.P. 1988, *Astron. J.*, **96**, 807.
- Worthey, G. 1993a, *Ap. J.*, **409**, 530. (Erratum in **418**, 947).
- Worthey, G. 1993b, *Ap. J. Lett.*, **415**, L91.
- Worthey, G. 1994, *Ap. J. Suppl.*, **95**, 107.